

BIODENTAL ENGINEERING

R.M. Natal Jorge
Sónia M. Santos
João Manuel R.S. Tavares
Mário A.P. Vaz
J.C. Reis Campos
EDITORS

PROCEEDINGS OF THE I INTERNATIONAL CONFERENCE ON BIODENTAL ENGINEERING,
PORTO, PORTUGAL, 26–27 JUNE 2009

Biodental Engineering

Editors

R.M. Natal Jorge

Sónia M. Santos

João Manuel R.S. Tavares

Mário A.P. Vaz

*Faculdade de Engenharia da Universidade do Porto
Porto, Portugal*

J.C. Reis Campos

*Faculdade de Medicina Dentária da Universidade do Porto
Porto, Portugal*



CRC Press

Taylor & Francis Group

Boca Raton London New York Leiden

CRC Press is an imprint of the
Taylor & Francis Group, an **informa** business

A BALKEMA BOOK

CRC Press/Balkema is an imprint of the Taylor & Francis Group, an informa business

© 2010 Taylor & Francis Group, London, UK

Typeset by Vikatan Publishing Solutions (P) Ltd., Chennai, India

Printed and bound in Great Britain by Antony Rowe, (A CPI Group Company), Chippenham, Wiltshire

All rights reserved. No part of this publication or the information contained herein may be reproduced, stored in a retrieval system, or transmitted in any form or by any means, electronic, mechanical, by photocopying, recording or otherwise, without written prior permission from the publisher.

Although all care is taken to ensure integrity and the quality of this publication and the information herein, no responsibility is assumed by the publishers nor the author for any damage to the property or persons as a result of operation or use of this publication and/or the information contained herein.

Published by: CRC Press/Balkema

P.O. Box 447, 2300 AK Leiden, The Netherlands

e-mail: Pub.NL@taylorandfrancis.com

www.crcpress.com – www.taylorandfrancis.co.uk – www.balkema.nl

ISBN: 978-0-415-57394-8 (Hbk)

ISBN: 978-0-203-85519-5 (Ebook)

Table of contents

| | |
|--|----|
| Acknowledgements | IX |
| Preface | XI |
| <i>Keynote papers</i> | |
| Collecting research data from clinical practice: How can informatics help? <i>T.K.L. Schleyer</i> | 3 |
| Human temporomandibular joint simulation <i>A. Pérez del Palomar & M. Doblaré</i> | 11 |
| <i>Regular papers</i> | |
| Biomechanical study of changes in buccal bone structure induced by expansion screw <i>I. Braga, D. Rocha, P. Filgueiras, E. Las Casas, R. Andrade, R. Natal Jorge & P.A.L.S. Martins</i> | 17 |
| Simulation of the behavior of mandibular periimplant bone with a remodeling model <i>J. Ojeda, J. Martínez-Reina & J. Mayo</i> | 23 |
| Damage detection in a human premolar tooth from image processing to finite element analysis <i>U. Andreaus, M. Colloca & D. Iacoviello</i> | 29 |
| Fracture behaviour of some heat curing dental resins <i>B. Ghiban, N. Ghiban, A. Ghiban, C.M. Bortun, N. Faur & A. Cernescu</i> | 35 |
| Effect of the material of the prefabricated post on restored premolars <i>P.J. Rodríguez-Cervantes, C. González-Lluch, J.L. Sancho-Bru, A. Barjau-Escribano, A. Pérez-González & L. Forner-Navarro</i> | 41 |
| Simulation of the bone filling of a dental alveolus <i>M.S. Commisso, J. Martínez-Reina & J. Mayo</i> | 47 |
| Histological evaluation of pulp tissue and periodontal regeneration in autogenous tooth transplantation <i>M.M. Ferreira, E.V. Carrilho, L. Carvalho & M.F. Botelho</i> | 53 |
| Methods for assessing dental wear in bruxism <i>A. Batista Meireles, T. Pereira Machado Cornacchia, E.B. Las Casas, F. de Souza Bastos, G.C. de Godoy, F. dos Santos Marques, P. Lilles Drews Jr., A. Alves Neto & M.F. Montenegro Campos</i> | 59 |
| Three dimensional skeletal muscle tissue modeling <i>Y.T. Lu, H.X. Zhu, J. Middleton, S. Richmond, L. Beldie & B. Walker</i> | 65 |
| New formulations for space provision and bone regeneration <i>P. Palma, S. Matos, J. Ramos, F. Guerra, H. Figueiredo & J. Kauser</i> | 71 |
| An automatic morphometrics data extraction method in dental X-ray image <i>L.A.P. Neves, P.H.M. Lira & G.A. Giraldi</i> | 77 |

| | |
|---|-----|
| Risk of failure at the cement-enamel junction of a human premolar tooth <i>U. Andreaus & M. Colloca</i> | 83 |
| A mechanobiological model for bone ingrowth on dental implants <i>M.A. Pérez, J.M. García-Aznar, M. Doblaré & P. Moreo</i> | 89 |
| Optical behavior of two dental bleaching agents irradiated with different wavelength <i>M.V. Lucas, G.R. Sousa & M. Pinotti</i> | 95 |
| Influence of Boroxide Bioactive Bioglasses (BBB) on osteoblast viability <i>P. Valério, A.M. Góes, U. Karacayli, O. Gunduz, S. Salman, A. Zeki Sengil, S. Yilmaz, S. Agathopoulos & F. Nuzhet Oktar</i> | 99 |
| Effect of sintering temperature on mechanical properties and microstructure of zeolite (clinoptilolite) reinforced bovine hydroxyapatite (BHA) composites <i>U. Karacayli, O. Gunduz, S. Salman, L.S. Ozyegin, S. Agathopoulos, A. Zeki Sengil & F. Nuzhet Oktar</i> | 105 |
| The thickness of the cortical bone in different maxillae using medical images <i>E.M.M. Fonseca, M.J. Lima, J.K. Noronha & M.A.P. Vaz</i> | 109 |
| Glass-ionomer cements: A review of their engineering properties <i>J.W. Nicholson</i> | 113 |
| Computational analysis of thermal and mechanical behaviour of FGM-based (Ti/HA) endosseous dental implants in normal and overloading conditions – <i>A method for designing an FGM-based innovative dental implant</i> <i>G. Cevola</i> | 117 |
| Metal ceramic fixed partial denture – fracture resistance <i>P. Piloto, A. Alves, A. Correia, J.C. Reis Campos, J.C. Sampaio Fernandes, M.A.P. Vaz & N. Viriato</i> | 125 |
| Pre-school telediagnosis of dental problems: A teledentistry project <i>R. Amável, R. Cruz-Correia & J. Frias-Bulhosa</i> | 129 |
| The strain patterns of the mandible for different loadings and mouth apertures <i>A. Ramos, A. Completo, C. Relvas, J.A. Simões, M. Mesnard & A. Ballu</i> | 133 |
| Maxilla bone pre-surgical evaluation aided by 3D models obtained by Rapid Prototyping <i>L. Queijo, J. Rocha, L. Barreira, T. Barbosa, A. Ramos & M. San Juan</i> | 139 |
| A numerical framework for wound healing at the bone-dental implant interface <i>J.C. Vanegas A., N.S. Landinez P. & D.A. Garzón-Alvarado</i> | 145 |
| Evaluation of desinsertion strength of total prosthesis with an intra-oral transducer <i>M.H. Figueiral, P. Fonseca & C. Pereira-Leite</i> | 153 |
| Analysis of the orthodontic wire behavior through the computational numerical simulation <i>E.A. Ferreira, A.C. Cimini Jr., E.B. Las Casas & N.F. Rilo</i> | 157 |
| Characterization of polymerization reaction of self-curing dental cements using fibre optic sensors <i>N.J. Alberto, J.L. Pinto, L. Carvalho & R.N. Nogueira</i> | 161 |
| Clinical evaluation of implant retained overdentures: Biological complications <i>J. Galvão-Mendes, M.H. Figueiral, C. Leal Silva, A. Pinho & F. Morais-Branco</i> | 165 |
| Case study of a temporomandibular joint hypermobility in classical singing <i>F.M. Lã, M.P. Clemente, N. Rocha & J.C. Pinho</i> | 169 |
| The biomechanical challenge with angled implants <i>T. Coutinho Almeida, P. Ferrás Fernandes, J.C. Sampaio Fernandes, C. Leal Silva & A. Pinho</i> | 177 |

| | |
|---|-----|
| Biomechanical and clinical performance of a cantilevered tooth-implant fixed bridge <i>A.A. Sousa, J. Galvão-Mendes, P. Rocha-Almeida, A. Pinho & J.C. Sampaio Fernandes</i> | 181 |
| Evaluation of the displacements transmitted to a pig jaw, by orthodontic and orthopaedic devices <i>A.P. Botto, L. Carvalho, J. Monteiro, N.V. Ramos, M. Vaz, M.B. Hecke & J. Ustrell</i> | 185 |
| Comparison of bracket/arch friction for passive self-ligated and conventional brackets <i>A.R. Barros & L. Carvalho</i> | 189 |
| Evaluation of the quantity of MMA released by denture base resins <i>M. Costa, V. Seabra, A. Amaral & L. Carvalho</i> | 195 |
| Muscular and articular forces exerted on the human mandible <i>M. Mesnard, A. Ballu, A. Ramos, J.A. Simões, V.A. Lokhov & Y.I. Nyashin</i> | 199 |
| Stress distribution on cantilever dental prostheses <i>A. Correia, J.C. Sampaio Fernandes, J.C. Reis Campos, M. Vaz, N.V. Ramos & J.M. da Silva</i> | 205 |
| Clinical evaluation of implant-retained overdentures: Mechanical complications <i>J. Galvão-Mendes, P.J. Almeida, J.C. Reis Campos, C. Leal Silva & J.C. Sampaio Fernandes</i> | 209 |
| Bioactive nanohybrid scaffolds mimicking natural dentin xenotransplanted in immunodeficient mice <i>A. Vallés, E. Novella, M. Sancho, G. Gallego, M. Monleón & C. Carda</i> | 213 |
| Manufacturing and evaluation of the effectiveness of a new custom mouthpiece for wind instrumentists <i>D. Coimbra, A. Portela, J. Frias-Bulhosa, J. Cavalheiro & M. Vasconcelos</i> | 219 |
| Minor maxillofacial bone augmentation for dental prostheses implantation <i>A.I. Silva, C. Calado, J. Julião, M.C. Gaspar & F.V. Antunes</i> | 225 |
| Author index | 231 |

Metal ceramic fixed partial denture – fracture resistance

Paulo Piloto & Ana Alves

Applied Mechanics Department, Polytechnic Institute of Braganza, Braganza, Portugal

André Correia, J.C. Reis Campos & J.C. Sampaio Fernandes

Faculty of Dental Medicine, University of Porto, Porto, Portugal

Mário A.P. Vaz & Nuno Viriato

Mechanical Department, Faculty of Engineering, University of Porto, Porto, Portugal

ABSTRACT: Metal ceramic Fixed Partial Dentures (FPD) are suitable to increase fracture resistance presenting higher clinical longevity. This type of prosthesis is mainly used when a great number of teeth replacements are needed. The FPD under analysis is defined by a metallic infrastructure (titanium) and by a ceramic coating. The advantages of hybrid FPD lie in their predictable biomechanical behaviour, versatility and cost. The main disadvantage is related to aesthetic functionality. Karlsson (1986), Lindquist & Karlsson (1998) and Palmqvist (1993) quantified the life time for hybrid FPD, referring 10 years in service to be a survival of break point. The connector design is of great importance to improve smooth stress pattern in the region between teeth. This region is also restrained by biological and aesthetic reasons. Ceramic material presents elevated failure rate in FPD due to brittleness. This work intends to predict fracture resistance to different loading conditions, using a smeared fracture approach (continuous damage mechanics). Results agree well with experimental evidence.

1 INTRODUCTION

Despite the increase of all-ceramic fixed partial dentures, metal ceramic units continue to be used due to their clinical durability and biocompatibility. Ceramic fractures represent serious and costly problems in dentistry. Moreover, they pose an aesthetic and functional dilemma both for the patient and the dentist, Özcan (2003).

Considering the existence of two or more different materials, with different biomechanical properties (thermal and mechanical) and also the adherence between them (bond strength), it is expectable to foresee problems under clinical conditions.

Failure of the restoration is dependent on different several factors. Optimum clinical design should require knowledge of failure mechanism. Besides the previous mentioned factors affecting failure, adverse environmental conditions, such as moisture and other fluids may also contribute to decrease life of FPD. The presence of microcracks at surface should be the most important reason for ceramic failure, besides the existence of pores inside ceramic material.

This paper intends to analyze the brittle behaviour of ceramic material used on fixed partial dentures, using the concept of continuous damage

mechanics. In this concept, the smear of a crack or crush is predicted by the stress level determined by tension or compression, maintaining the continuity of the displacement field where the material became ineffective.

A three unit FPD consisting of two piles and a supported tooth is analyzed, when subjected to three different loading conditions over the pontic area on the top region of crown (L1—load type one considered as two point load at the cusps zone, L2—load type two considered as ring load at the top zone and L3—load type three considered as one point load located in the fossa zone), see Figure 1.

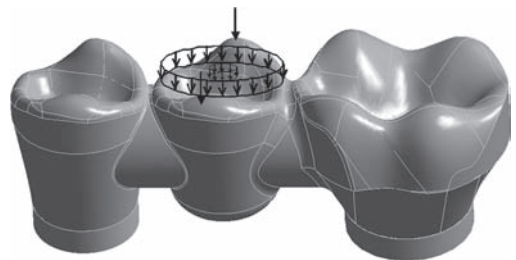


Figure 1. Three unit FPD and loading conditions, (L1, L2, L3).

All loads were applied orthogonal to the occlusal plane, using incremental procedure to predict smeared cracking and crushing.

The three unit FPD is made of a metallic infrastructure (titanium) and a ceramic coating, assuming perfect contact between them.

2 OBJECTIVES

The objective of this research is to predict damage on ceramic material, depending on load type and level. An incremental loading step was applied until the maximum load bearing was reached for each loading condition. Those different loading condition should represent a wide range of dally situations. The pattern of cracking and crushing should be determined. Cracking is the ultimate state condition under tension while crushing is represented by compressive stress state.

3 MATERIALS

Two different materials should be defined for numerical simulation of this metal-ceramic partial fixed denture. The adherence between them is not considered in this investigation, assuming perfect contact between both. The ceramic material should be considered as brittle, using adequate constitutive relations and the titanium should be considered as normal ductile metallic behaviour.

Ceramic present higher strength resistance in compression than in tension. Figure 2 represents the mechanical behaviour under uniaxial stress conditions, being the material capable of stress relieving under tension stress. This behaviour is normally used to increase numerical convergence.

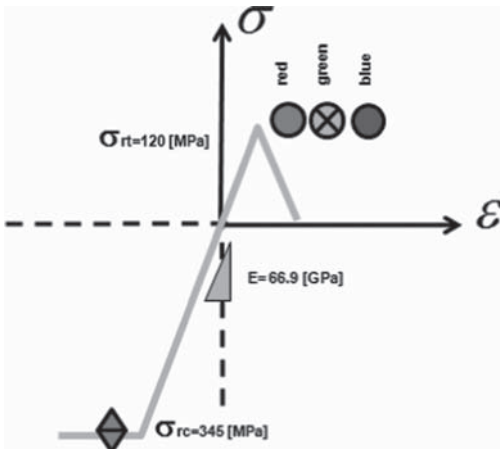


Figure 2. Stress – strain relation for ceramic material.

Material may undergo plastic behaviour under compression. Table 1 represents the material properties used together with failure mechanism, based on Willam and Warnke (1975) criteria.

Titanium alloy is considered as ductile material, which means that material presents linear elastic and may undergo plastic deformation, under tension and compression, see Figure 3. Strain values for ultimate stress may present values close to 20%.

Table 2 represents the mechanical material properties for tension and compression of titanium.

Table 1. Material model for ceramic material.

| Model | Property/Function | Value |
|------------------------------|-------------------------------------|------------|
| Linear (tension/compression) | Elastic modulus | 66.9 [GPa] |
| | Poisson coefficient | 0.29 |
| Non-linear (compression) | Strain | Stress |
| | 0 | 0 |
| | 0.005156 | 345 [MPa] |
| | 0.010000 | 345 [MPa] |
| Failure model | Shear transfer coef. (open crack) | 0.25 |
| | Shear transfer coef. (closed crack) | 0.90 |
| | Tensile cracking stress | 120 [MPa] |
| | Compressive crushing stress. | 345 [MPa] |
| | Stiffness mult. for cracked tensile | 1 |

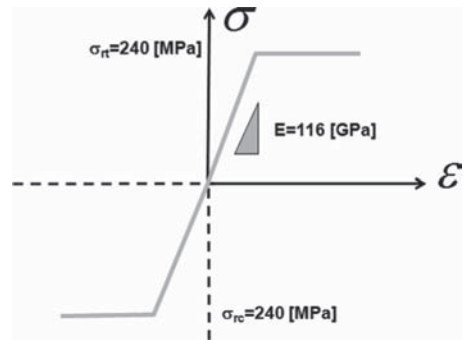


Figure 3. Stress – strain relation for titanium.

Table 2. Material model for titanium alloy material.

| Model | Property/Function | Value |
|------------------------------------|---------------------|-----------|
| Linear (ten. / compr.) | Elastic modulus | 116 [GPa] |
| | Poisson coefficient | 0.34 |
| Non-linear (tension / compression) | Strain | Stress |
| | 0 | 0 |
| | 0.002068 | 240 [MPa] |
| | 0.200000 | 240 [MPa] |

4 METHODS OF ANALYSIS

The geometry of this fixed partial denture was defined as parasolid format in Solidworks CAD software and then fully transferred to the analysis ANSYS software. The geometry is mathematically modified to finite solid 65 and solid 45 elements to represent ceramic and metallic material, respectively, see Figure 4.

The metal infrastructure is a bridge in cantilever supporting condition.

Solid 65 is a three dimensional finite element with eight nodes and eight integration points, with three degrees of freedom at each node (translations in the nodal x, y, and z directions). The most important feature of this element is that it can represent both linear and non-linear behaviour of the ceramics. For the linear stage, the ceramics is assumed to be an isotropic material up to cracking. For the non-linear part, the ceramics may undergo plasticity. Cracking may take place up to three orthogonal directions at each integration point. A crack may be developed in one plane and if subsequent tangential stress to the crack face are large enough, a second (or third) crack may also be developed (red, green and blue color circle outline), see Figure 5. If the crack has opened and then closed, the circle outline will have an X through it.

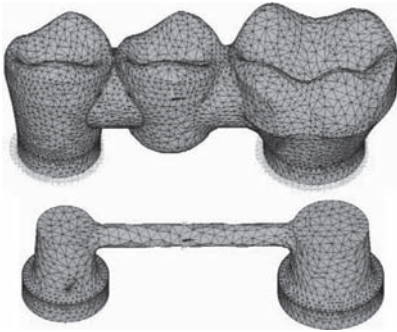


Figure 4. Unstructured finite element mesh with tetrahedrons. Complete mesh and metallic infrastructure.

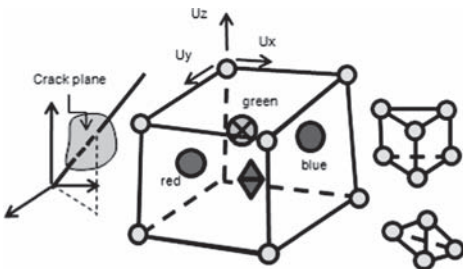


Figure 5. Finite solid 65 element.

Cracking is assumed to be spatially distributed over entire volume of element or volume attached to each integration point. The presence of a crack at an integration point is represented through modification of the stress-strain relations by introducing a plane of weakness in a direction normal to the crack face.

If the material fails at an integration point during uniaxial, biaxial, or triaxial compression, the material is assumed to crush at that point. In solid 65, crushing is defined as the complete deterioration of the structural integrity of the material and represented by an octahedron outline. Under conditions where crushing has occurred, material strength is assumed to have degraded to an extent such that the contribution to the stiffness of an element, at the integration point in question, can be ignored.

Solid 45 is a three dimensional finite element with almost the same characteristics as mentioned except for predicting cracking and crushing.

5 RESULTS

Load bearing resistance was determined for each loading condition. Table 3 resumes the ultimate load for support equilibrium. After that load level it is no longer possible to sustain equilibrium and the 3 unit FPD is considered damaged.

Progressive degradation lead to crack initiation and growth, as represented in Figures 6–8.

For load case L1, cracking is initiated next to the loading zone (cusps) and progressive damage also stars at the bottom of the abutments, in the neighbourhood to the bottom ceramic material.

The stress field is strongly dependent on fracture prediction, because material is losing resistance near cracks and crushed ceramic material.

For Load case L2, cracking is initiated next to the left abutment with progressive damage in the neighbourhood to the bottom ceramic material.

The stress field is similar to the resultant stress field for load case L1, and is also dependent on fracture progressive damage.

For Load case L3, cracking is initiated at the bottom of the abutments, with progressive collapse in the loading zone and also in the connecting bridge element, which represents traditional collapsing mode, as reported by different authors, Tsumita et al. (2007).

Table 3. Fracture resistance.

| Loading | Ultimate load |
|---------|---------------|
| L1 | 128 [N] |
| L2 | 201 [N] |
| L3 | 514 [N] |

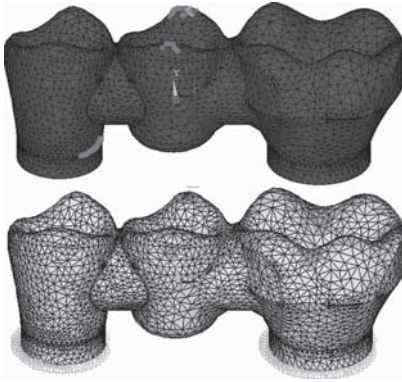


Figure 6. Ultimate limit state condition of FPD to load type 1 – LT1. Fracture prediction and longitudinal stress field.

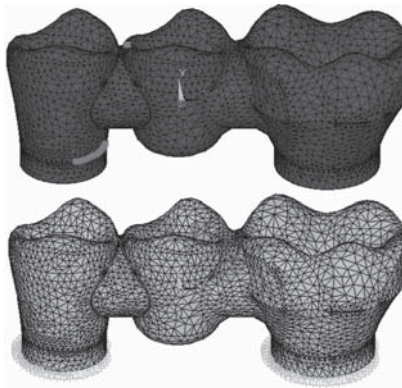


Figure 7. Ultimate limit state condition of FPD to load type 2 – LT2. Fracture prediction and longitudinal stress field.

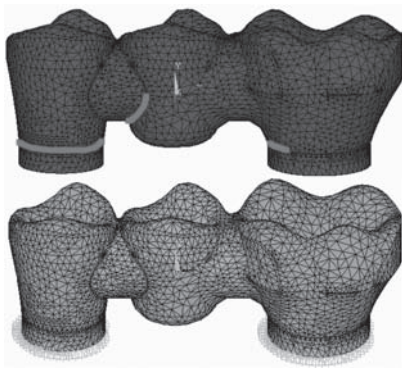


Figure 8. Ultimate limit state condition of FPD to load type 3 – LT3. Fracture prediction and longitudinal stress field.

The stress field presents two well defined compressive and tensile zones.

The connection bridge presents different design near central tooth (pontic). The rounded shape on the right contrast with the sharp geometry on the left, which is responsible for increasing the stress level and simultaneously with progressive failure.

6 CONCLUSIONS

There is consistent epidemiological evidence that mechanical failure of a dental prosthesis occurs after a certain number of service years. In case of prosthodontic restoration, ceramics cannot be added intraorally due to processing conditions. Replacement of a failed fixed partial denture is not a practical solution, reason why this type of prosthesis should be carefully design for maximum life cycle, Özcan (2003).

The most frequent reasons for ceramic failures are related to progressive cracking. Sharp shape geometry should be avoided to decrease maximum stress level.

Three different loading conditions were tested, leading to different fracture resistance. Load case L1 presented smaller fracture resistance due to localized effect of the applied force. Progressive collapsing near the abutment was revealed. Load case L2 presented higher fracture resistance, but failure occurred in the same location as load L1. This is mainly due to the similar resultant stress field. Load case L3 revealed maximum fracture resistance, with typical collapsing mode.

REFERENCES

- Karlsson, S. "A clinical evaluation of fixed bridges, 10 years following insertion"; *J Oral Rehabil* 1986; 13: 423–32.
- Lindquist, E. & Karlsson, S. "Success rate and failures for fixed partial dentures after 20 years of service: part I."; *Int J Prosthodont* 1998; 11: 133–8.
- Özcan, M. "Fracture reasons in ceramic-fused-to-metal restorations"; *J Oral Rehabil* 2003; 30: 265–9.
- Palmqvist, S. & Swartz, B. "Artificial crowns and fixed partial dentures 18 to 23 years after placement"; *Int J Prosthodont*, 1993; 6: 279–85.
- Tsumita, M., Kokubo, Y., Vult von Steyern, P. & Fukushima, S. "Effect of framework shape on the fracture strength of implant-supported all-ceramic fixed partial dentures in the molar region"; *Journal of prosthodontics: official journal of the American College of Prosthodontists*. 2008 Jun;17(4): 274–85.
- Willam, K.J. & Warnke, E.D. "Constitutive Model for the Triaxial Behavior of Concrete", *Proceedings, International Association for Bridge and Structural Engineering*, Vol. 19, ISMES, Bergamo, Italy, p. 174 (1975).